Development of an acoustic material property database and universal airflow resistivity model

R.K. Dunne[a,*], D.A. Desai[a] and P.S. Heyns[b]

[a]Department of Mechanical and Automation Engineering, Faculty of Engineering and the Built Environment, Tshwane University of Technology, Pretoria 0001, South Africa
[b]Department of Mechanical & Aeronautical Engineering, Faculty of Engineering, Built Environment & IT, University of Pretoria, Pretoria 0001, South Africa

*Corresponding author.dunnerk@tut.ac.za

Abstract

The importance of accurate airflow resistivity predictive models and a subsequent comprehensive database of acoustic material properties for designers cannot be underestimated. With the advances in Finite Element Analysis software, the development of physical prototypes for preliminary testing is becoming obsolete. This is due to the limited resources available and pressure on designers by industry to accomplish tasks in shorter time frames. Therefore, the primary purpose of this research was to develop a comprehensive database of acoustic material properties such as airflow resistivity, bulk density, fibre density and fibre diameter, for designers to draw from, since there is no comprehensive database currently in the literature. Secondly, this research attempts to provide a comprehensive list of available airflow resistivity predictive models, for the designer's convenience. Furthermore, this research attempts to evaluate the accuracy of the available models by benchmarking each model against experimental data, this will allow for the correct implementation of the model. Finally, this research proposes a universal airflow resistivity predictive empirical model, this is necessary since the current available models are limited in their predictive range. Based on this model, it was found that the predicted percentage error of the airflow resistivity had no visible correlation with the bulk density and fibre diameter. Thus, the range (i.e. the bulk density and fibre diameter range) did not influence the percentage error between the measured and predicted airflow resistivity. Interestingly, it was found that the majority of high percentage errors that occurred came from inaccuracies in the data presented in the available literature. Finally, it was determined that further research to improve the body of knowledge is required.

Keywords: Airflow resistivity; Database; Predictive models; Acoustic material properties

1. Introduction

The purpose of this study was to provide designers with a resource that can aid in their development and implementation of new sound absorbing products. This was thought necessary since there has been much development in Finite Element Analysis (FEA) over the years, and designers are utilizing these software packages for preliminary prototyping of new products. Without an adequate database of material properties, accurate FEA models become futile in the case of limited or no experimental testing to find material properties. Wu, did attempt to produce a materials database, however, this database is rudimentary and only contains several commonly used materials [1]. Furthermore, there is no single comprehensive resource or database to which designers can turn to for acoustic material properties. Also, the available literature does not provide a sufficient study on the availability and accuracy of mathematical models for the prediction of airflow resistivity, which is necessary to utilize if material properties and experimental testing facilities are not available. Therefore, the primary focus of this study was to develop a comprehensive database of acoustic material properties. This was particularly challenging since in recent years there has been much development of environmentally friendly materials, of which there can be nearly countless variations. Secondly, this study attempted to provide a comprehensive list of available airflow resistivity predictive models. Furthermore, this study attempted to evaluate the accuracy of the available models by benchmarking each model against experimental data. Finally, this study attempted to provide a universal airflow resistivity predictive model. The use of the word universal implies that the developed model is suitable for application on any fibre type.

2. Airflow resistivity models of porous fibrous materials

Over the years several mathematical and empirical models, for the prediction of the airflow resistivity of porous fibrous materials, have been developed. These models are particularly useful during rapid prototyping and/or when experimental testing facilities are not available. This is advantageous since acoustic test equipment and experimental testing can be expensive both in cost and time. The airflow resistivity is an important property that is needed when using empirical-based models for the prediction of the sound absorption coefficient of poroelastic materials. The sound absorption coefficient is of particular importance, for the accurate determination of the sound pressure levels (SPL's) within a vehicle cabin, since the vehicle trims, which for the most part act as sound absorbers, require the input of material sound-absorbing data [2]. However, this can be detrimental if the available models, being used for predicting acoustic properties, are not reliable in terms of their accuracy. Therefore, when modelling a vehicle cabin it is of utmost importance to have the correct sound absorption coefficient of the material for accurate prediction in FEA software. If the predictive models, for the sound absorption coefficient, have a low-accuracy this could cause delays in product development lead times. This ultimately affects the manufacturing company's competitiveness and also leads to higher developmental costs. However, if mathematical and/or empirical models with high accuracy are available and their effective working range is well defined then their use in rapid prototyping can be implemented safely, this can be very beneficial.

A thorough literature review was conducted to determine the number of airflow resistivity models that have been developed. From the literature, the following airflow resistivity models were found as listed in Table 1. Through the literature search, 24 airflow resistivity models were found. These models were developed for the prediction of the airflow resistivity for varies materials. A number of the models did not specify their working range. This makes it difficult to implement in real-world problems since the accuracy of the model will be directly related to the material properties. Never the less, the accuracy can be determined if the model is benchmarked against reliable experimental data.

2.1. Accuracy determination of predictive models

Since the accuracy of these models are so important for the prediction of the sound absorption coefficient and ultimately the SPL's in FEA software, the authors thought it

Table 1
Airflow resistivity models.

Models	Airflow Resistivity	Fibre Type	Bulk Density Range(kg/m^3)	Fibre Diameter Range(μm)	Year	References
Langmuir	$\sigma = \frac{16\mu(1-\varepsilon)}{d^2\left[-\ln(1-\varepsilon)-1.5+2(1-\varepsilon)-\frac{(1-\varepsilon)^2}{2}\right]}$				1942	[3,4]
Kozeny-Carman	$\sigma = 180\mu\frac{(1-\varepsilon)^2}{d^2\varepsilon^3}$	Granular Media			1956	[5]
Bies	$\sigma = \frac{3.18\times10^{-9}\rho_B^{1.53}}{d^2}$	Fibre Glass	$23 \le \rho_B \le 74$	$d < 15$	1971	[6,7,8]
Bies-Hansen-1	$\sigma = 27.3\left(\frac{\rho_B}{d_f}\right)^{1.53}\left(\frac{\mu}{d^2}\right)$	Glass fibre and rockwool	$23 \le \rho_B \le 74$	$d < 15$	1984	[8,9]
Ballagh	$\sigma = 490\frac{\rho_B^{1.61}}{d}$	Sheep's Wool	$13 \le \rho_B \le 80$	$22 \le d \le 35$	1996	[8,10]
Tarnow	$\sigma = \frac{16\mu(1-\varepsilon)}{d^2[-1.28\ln(1-\varepsilon)+0.526-2\varepsilon]}$	Glass Wool			1996	[4,11]
Kirby-Cummings-1	$\sigma = 1.857\rho_B^{1.687}$	A-Glass			1998	[12]
Kirby-Cummings-2	$\sigma = 5.774\rho_B^{1.792}$	E-Glass			1998	[12]
Kirby-Cummings-3	$\sigma = 3.012\rho_B^{1.761}$	Basalt wool			1998	[12]
Sullivan-1	$\sigma = 42.24\mu\frac{(1-\varepsilon)^{1.531}}{d^2\varepsilon^3}$	Glass Fibre Perpendicular to Flow		$12 \le d \le 20$	As reported in Mechel, 2002	[13]
Sullivan-2	$\sigma = 27.2\mu\frac{(1-\varepsilon)^{1.296}}{d^2\varepsilon^3}$	Glass Fibre Perpendicular to Flow		$40 \le d \le 60$	As reported in Mechel, 2002	[13]
Sullivan-3	$\sigma = \frac{16\mu}{d^2}\left[\frac{0.55(1-\varepsilon)^{\frac{4}{3}}}{\varepsilon}+\frac{\sqrt{2}(1-\varepsilon)^2}{\varepsilon^2}\right]$	Glass fibres, Random Orientation			As reported in Mechel, 2002	[13]
Sullivan-4	$\sigma = 12.8\mu\frac{(1-\varepsilon)^{1.42}}{d^2}$	Glass Fibre, Random Fibre Diameter Distribution and Random Fibre Orientation			As reported in Mechel, 2002	[13]
Sullivan-5	$\sigma = 17.6\mu\frac{(1-\varepsilon)^{1.59}}{d^2}$	Mineral Fibre, Random Fibre Diameter Distribution and Random Fibre Orientation			As reported in Mechel, 2002	[13]
Bies-Hansen-2	$\sigma = 27.3(1-\varepsilon)^{1.53}\left(\frac{\mu}{d^2}\right)$	Glass Fibre			2003	[14]
Garai-Pompoli	$\sigma = \frac{2.83\times10^{-8}\rho_B^{1.404}}{d^2}$	Polyester Fibre	$12 \le \rho_B \le 60$	$18 \le d \le 48$	2005	[4,7]
Kino-Ueno	$\sigma = \frac{1.5\times10^{-8}\rho_B^{1.51}}{d^2}$	Polyester Fibre	$35.9 \le \rho_B \le 64.4$	$13.5 \le d \le 39.1$	2007	[15]
Modified Ballagh	$\sigma = 490\frac{\left(\rho_B\frac{\rho_{wool}}{\rho_f}\right)^{1.61}}{d}$				2009	[14]
Ramis	$\sigma = 1.86\rho_B^{1.9}$	Kenaf Fibre	$47 \le \rho_B \le 132$		2010	[16]
Yilmaz	$\sigma = 16400 + 367000\frac{\rho_B^{1.6}}{\rho_f^{1.6}}$	Monofibre nonwovens			2011	[17]
Manning-Panneton (Thermal Bonded)	$\sigma = \frac{1.94\times10^{-8}\rho_B^{1.516}}{d^2}$	Shoddy Fibre	$66 \le \rho_B \le 83$	$11 \le d \le 75$	2013	[18]
Manning-Panneton (Mechanically Bonded)	$\sigma = \frac{2.03\times10^{-8}\rho_B^{1.485}}{d^2}$	Shoddy Fibre	$66 \le \rho_B \le 83$	$11 \le d \le 75$	2013	[18]
Manning-Panneton (Resin Bonded)	$\sigma = \frac{3.61\times10^{-8}\rho_B^{1.804}}{d^2}$	Shoddy Fibre	$66 \le \rho_B \le 83$	$11 \le d \le 75$	2013	[18]
Pelegrinis	$\sigma = \frac{180\mu}{\rho_f^2}\left(\frac{\rho_B}{d_f}\right)^2$	Polyester Fibre	$22.9 \le \rho_B \le 40.1$		2016	[19]
Yang	$\sigma = \frac{1.3395\times10^{-8}\rho_B^{1.585}}{d^2}$	Polyester nonwovens	$16.93 \le \rho_B \le 44$	$d = 15.94$	2018	[4]

where $\rho_B$is the bulk density of the poroelastic material, ρ_f is the fibre density, d_f is the fibre diameter, ε is the porosity of the poroelastic material, η is the dynamic viscosity of the fluid.

necessary to benchmark all the models in Table 1 against experimental data. The airflow resistivity models were benchmarked using a variety of different fibrous materials, including both synthetic and natural fibres, with various material properties. The materials used to benchmark the airflow resistivity models were selected from Table 3. Note, not all the materials in Table 3 were used but rather a subset of the most reliable data was used. The reliability criteria was based on the material properties that were given. Furthermore, these material properties, such as fibre diameter, were benchmarked against established data such as that given in [20], to establish their reliability. The order of the models in the below table follows the same order as the above table.

It should be noted that the average percentage error in Table 2, was calculated using:

$$A_{PE} = \frac{\left|\sum PE_{meas} - \sum PE_{pred}\right|}{PE_{meas}} \tag{1}$$

where A_{PE} is the average percentage error, PE_{meas} is the measured percentage error and PE_{pred} is the predicted percentage error. It can be seen from Table 2 that out of the 24 models listed only five of the models predicted the airflow resistivity with reasonable accuracy. This result was not expected. Possible reasons for the inability of the listed models to accurately predict the airflow resistivity could be that many of the models were developed using a very specific range of materials, and hence can only perform in that range. Also, it could be the case that some of the models did not go through a rigours verification process using independent data. This can lead to the model's capability being severely limited. Which is the case for many of the models listed in Table 2.

It can be seen, in Table 2, that the Bies model predicted the airflow resistivity of the kapok material extremely accurately.

The authors of this data (the kapok data) may have originally used the Bies model to predict the airflow resistivity for their research, hence, the low percentage error obtained in Table 2.

2.2. Acoustic material database

The acoustic materials database presented below in Table 3, Table 4 were compiled using a variety of sources such as journal articles, book chapters, dissertations and theses. Table 3 is arranged in the order of lowest airflow resistivity to highest airflow resistivity.

The predicted glass wool fibre diameters listed in Table 3, were acquired from a figure in [6], that relates airflow resistivity to fibre diameter. This figure was developed specifically for glass fibres, hence the reason for it being used. These values were cross-referenced using the Bies model, which predicted the values within an average percentage error of 4.6%.

It should be noted that some of the fibre densities given in Table 2, were determined by making use of the porosity. Hence, higher than expected densities may occur due to the manufacturing process used and the type of binding matrix applied to the composite.

It has been noted by Bies and Hansen, that a decrease in fibre diameter results in an increase of the flow resistivity and an increase in the sound absorption of the material [9]. This is evident in Table 3. However, the data presented by [19], shows an increase in the airflow resistivity with an increase in fibre diameter. Caution should be exercised with such data

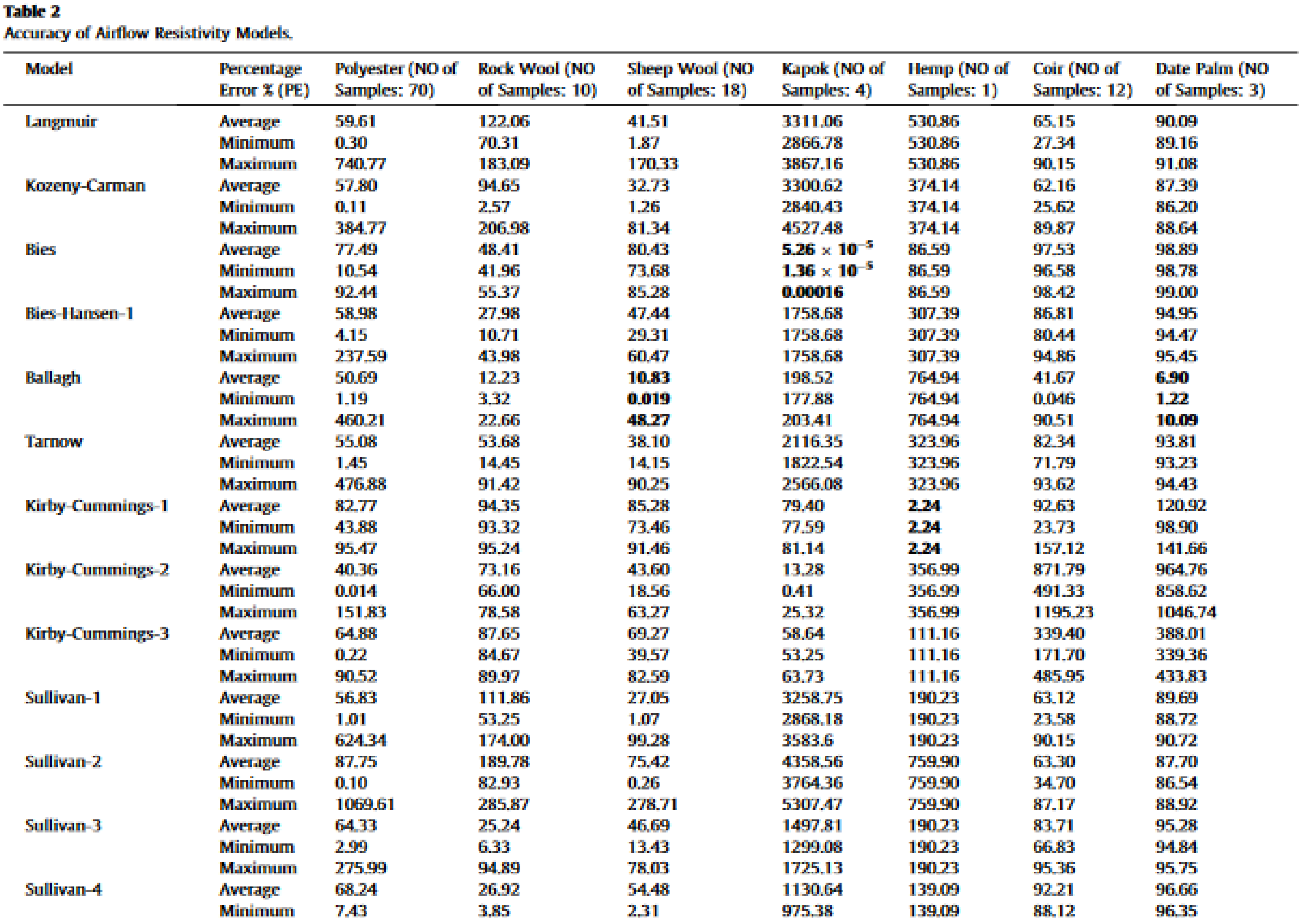

Table 2

Accuracy of Airflow Resistivity Models.

Model	Percentage Error % (PE)	Polyester (NO of Samples: 70)	Rock Wool (NO of Samples: 10)	Sheep Wool (NO of Samples: 18)	Kapok (NO of Samples: 4)	Hemp (NO of Samples: 1)	Coir (NO of Samples: 12)	Date Palm (NO of Samples: 3)
Langmuir	Average	59.61	122.06	41.51	3311.06	530.86	65.15	90.09
	Minimum	0.30	70.31	1.87	2866.78	530.86	27.34	89.16
	Maximum	740.77	183.09	170.33	3867.16	530.86	90.15	91.08
Kozeny-Carman	Average	57.80	94.65	32.73	3300.62	374.14	62.16	87.39
	Minimum	0.11	2.57	1.26	2840.43	374.14	25.62	86.20
	Maximum	384.77	206.98	81.34	4527.48	374.14	89.87	88.64
Bies	Average	77.49	48.41	80.43	**5.26×10^{-5}**	86.59	97.53	98.89
	Minimum	10.54	41.96	73.68	**1.36×10^{-5}**	86.59	96.58	98.78
	Maximum	92.44	55.37	85.28	**0.00016**	86.59	98.42	99.00
Bies-Hansen-1	Average	58.98	27.98	47.44	1758.68	307.39	86.81	94.95
	Minimum	4.15	10.71	29.31	1758.68	307.39	80.44	94.47
	Maximum	237.59	43.98	60.47	1758.68	307.39	94.86	95.45
Ballagh	Average	50.69	12.23	**10.83**	198.52	764.94	41.67	**6.90**
	Minimum	1.19	3.32	**0.019**	177.88	764.94	0.046	**1.22**
	Maximum	460.21	22.66	**48.27**	203.41	764.94	90.51	**10.09**
Tarnow	Average	55.08	53.68	38.10	2116.35	323.96	82.34	93.81
	Minimum	1.45	14.45	14.15	1822.54	323.96	71.79	93.23
	Maximum	476.88	91.42	90.25	2566.08	323.96	93.62	94.43
Kirby-Cummings-1	Average	82.77	94.35	85.28	79.40	**2.24**	92.63	120.92
	Minimum	43.88	93.32	73.46	77.59	**2.24**	23.73	98.90
	Maximum	95.47	95.24	91.46	81.14	**2.24**	157.12	141.66
Kirby-Cummings-2	Average	40.36	73.16	43.60	13.28	356.99	871.79	964.76
	Minimum	0.014	66.00	18.56	0.41	356.99	491.33	858.62
	Maximum	151.83	78.58	63.27	25.32	356.99	1195.23	1046.74
Kirby-Cummings-3	Average	64.88	87.65	69.27	58.64	111.16	339.40	388.01
	Minimum	0.22	84.67	39.57	53.25	111.16	171.70	339.36
	Maximum	90.52	89.97	82.59	63.73	111.16	485.95	433.83
Sullivan-1	Average	56.83	111.86	27.05	3258.75	190.23	63.12	89.69
	Minimum	1.01	53.25	1.07	2868.18	190.23	23.58	88.72
	Maximum	624.34	174.00	99.28	3583.6	190.23	90.15	90.72
Sullivan-2	Average	87.75	189.78	75.42	4358.56	759.90	63.30	87.70
	Minimum	0.10	82.93	0.26	3764.36	759.90	34.70	86.54
	Maximum	1069.61	285.87	278.71	5307.47	759.90	87.17	88.92
Sullivan-3	Average	64.33	25.24	46.69	1497.81	190.23	83.71	95.28
	Minimum	2.99	6.33	13.43	1299.08	190.23	66.83	94.84
	Maximum	275.99	94.89	78.03	1725.13	190.23	95.36	95.75
Sullivan-4	Average	68.24	26.92	54.48	1130.64	139.09	92.21	96.66
	Minimum	7.43	3.85	2.31	975.38	139.09	88.12	96.35

	Maximum	218.93	95.60	81.08	1403.53	139.09	96.43	97.00
Sullivan-5	Average	73.90	41.35	68.63	901.038	81.13	92.37	97.06
	Minimum	31.55	18.72	38.60	788.56	81.13	88.78	96.79
	Maximum	125.51	97.23	88.11	1039.01	81.13	97.05	97.36
Bies-Hansen-2	Average	61.25	32.55	40.86	1767.99	246.74	86.67	94.67
	Minimum	14.13	6.39	12.50	1549.69	246.74	80.13	94.17
	Maximum	342.34	94.34	75.69	2080.47	246.74	94.52	95.20
Garai-Pompoli	Average	61.60	178.25	24.79	522.10	914.30	87.64	94.14
	Minimum	0.49	141.28	0.46	479.75	914.30	82.67	93.59
	Maximum	698.96	227.50	77.57	565.83	914.30	92.57	94.73
Kino-Ueno	Average	53.34	143.37	13.83	371.70	780.12	88.33	94.75
	Minimum	0.66	110.53	1.65	371.70	780.12	83.85	94.25
	Maximum	541.97	173.80	30.58	371.70	780.12	92.54	95.27
Modified Ballagh	Average	**39.01**	**8.69**	10.83	2124.19	595.48	196.25	74.71
	Minimum	**0.73**	**2.60**	0.019	2027.47	595.48	2.75	57.30
	Maximum	**415.17**	**14.06**	48.27	2222.91	595.48	321.46	91.12
Ramis	Average	64.96	86.60	69.19	61.78	124.61	415.40	438.37
	Minimum	0.57	81.80	29.41	53.68	124.61	196.42	384.71
	Maximum	90.57	89.97	83.48	69.15	124.61	585.35	488.92
Yilmaz	Average	577.59	43.65	919.35	1919.09	1184.97	1255.25	2146.10
	Minimum	0.50	13.34	0.88	793.95	1184.97	737.91	1922.19
	Maximum	2316.73	70.48	2198.66	3561.82	1184.97	1851.04	2357.00
Manning-Panneton (Thermal Bonded)	Average	62.73	197.67	17.75	486.19	977.62	85.85	93.59
	Minimum	0.18	158.06	0.54	481.70	977.62	80.41	93.00
	Maximum	690.65	236.27	55.69	490.71	977.62	91.01	94.23
Manning-Panneton (Mechanically Bonded)	Average	58.47	175.30	16.28	461.57	898.83	87.15	94.11
	Minimum	1.60	139.78	1.56	447.77	898.83	82.15	93.56
	Maximum	642.42	213.80	52.18	475.53	898.83	91.96	94.70
Manning-Panneton (Resin Bonded)	Average	642.93	1661.61	430.97	2395.00	6086.94	**27.16**	60.32
	Minimum	61.25	1296.07	268.86	2033.44	6086.94	**1.84**	56.60
	Maximum	3923.88	2149.35	620.15	2782.78	6086.94	**37.87**	64.28
Pelegrinis	Average	55.39	88.48	45.30	2858.61	443.09	64.84	90.46
	Minimum	2.89	32.74	5.43	2145.23	443.09	38.14	89.57
	Maximum	284.45	172.28	65.81	3662.76	443.09	91.86	91.41
Yang	Average	53.76	149.92	12.74	365.49	801.28	87.77	94.57
	Minimum	0.071	115.00	1.61	356.58	801.28	83.06	94.06
	Maximum	547.84	178.25	31.41	374.48	801.28	92.05	95.11

Table 3
Database of Experimental data.

Material Type	Thickness(mm)	Airflow Resistivity($Pa.s/m^2$)	Bulk Density(kg/m^3)	Fibre Density(kg/m^3)	Mean Fibre Diameter(μm)	Predicted Fibre Diameter(μm)	Reference
Natural Coconut Fibre	42	1200	83				[21]
	29	1900	100				[21]
	19	2600	128				[21]
	50	1500	60	1250	250		[22]
	100	1500	60	1250	250		[22]
	20	1680	99	800	250		[23]
	42	1800	83	1250	250		[23]
	29	2300	100	1250	250		[23]
	40	2910	100	541	263		[24]
	19	3100	128	1250	250		[23]
	20	3150	100	541	263		[24]
	45	4535	130	541	263		[24]
	20	4566	130	537	273		[25]
	35	4680	130	541	263		[26]
	25	4810	130	541	263		[26]
	30	5910	153	537	273		[25]
	45	6298	159	537	273		[25]
Coir Fibre (Industrial Prepared)	50	1359	87	821	252		[22]
	35	1440	90	821	252		[22]
	20	1680	99	821	252		[22]
Cotton	50	22,342	40.5	1500	13.5		[27]
Date Palm Fibre	40	879	65	930	420		[28]
	30	956	65	930	420		[28]
	20	1068	65	930	420		[28]
	40	1535	100	930	465		[24]
	20	1785	100	930	465		[24]
Glass Wool	52.5	6000	20	2500		7	[6,29]
	53.5	6600	20.2	2500		6.9	[6,29]
	54	6900	22.2	2500		7.2	[6,29]
	50	9600	18	2500	5.2		[30]
	25	11,900	28	2500		6.7	[6,31]
	25	12,300	28	2500		6.5	[6,29]
	25	13,600	32.2	2500		7.2	[6,29]
	25	16,500	33.8	2500		6.8	[6,29]
	25	16,800	31.8	2500		6.3	[6,29]

	26	17,800	37.9	2500		6.9	[6,29]
	52	18,600	43.6	2500		7.5	[6,29]
	52	19,100	47.2	2500		8	[6,29]
	24.5	21,500	41.7	2500		6.9	[6,31]
	50	28,000	76	2500		9.5	[30]
	25	29,000	52.6	2500		7	[6,31]
	1.9	29,600	91.5	2500		16	[6,32]
	100	40,000	130	2500		8	[6,33]
	10	44,600	81.2	2500		7.9	[6,29]
	17.9	48,600	102.2	2500		9	[6,32]
	10	49,000	81.2	2500		7.5	[6,31]
	14.3	52,900	78	2500		6.3	[6,32]
	26.5	53,100	90.9	2500		8	[6,29]
	14	53,300	84.7	2500		7.3	[6,31]
	27	54,600	87.8	2500		7.3	[6,29]
	27	55,200	85.1	2500		7.2	[6,29]
	13.9	63,100	75	2500		6.3	[6,32]
	8	63,900	102.2	2500		7.4	[6,29]
	14	69,900	101.2	2500		7.5	[6,31]
	13.3	70,600	92.9	2500		9	[6,32]
	8	72,900	102.4	2500		7.4	[6,29]
	30	98,000	129	2500	7.5		[30]
Hemp Fibre	30	1400	50	1500	22		[22,34]
Jute Fibre	25.4	20,088	336	1400			[22]
Kapok Fibre	60	478.899	10	370	15		[35]
	60	890.562	15	370	15		[35]
	60	1382.995	20	370	15		[35]
	60	2571.817	30	370	15		[35]
Kenaf Fibre	60	2700	50	1400			[22]
	40	3500	100	1400			[22]
	60	3500	100	1400			[22]
	18	4045	79	1400			[22]
	50	4233.57	196	1400	12.81		[36,37]
	22	4710	86	1400			[22]
	18	4798	125	1400			[22]
	42	5226	60	1400			[22]
	15	5662	73	1400			[22]
	73	5712	70	1400			[22]

	19	6167	120	1400		[22]
	82	6628	62	1400		[22]
	50	7387.23	241	1400	12.81	[36,37]
	68	8630	65	1400		[22]
	44	17,649	47	1400		[22]
	28	20,598	70	1400		[22]
	17	30,000	132	1400		[22]
Polyester	200	700	22.8	1380	20.2	[19]
	200	800	24.4	1380	20.2	[19]
	130	880	14	1380	33	[7]
	112	912	13	1380	33	[7]
	123	922	12	1380	33	[7]
	76	1101	15	1380	33	[7]
	103	1110	14	1380	33	[7]
	135	1192	15	1380	33	[7]
	200	1200	32.9	1380	20.2	[19]
	89	1363	20	1380	33	[7]
	100	1423	15	1380	33	[7]
	82	1465	17	1380	33	[7]
	200	1600	22.8	1380	24.8	[19]
	77	1700	18	1380	33	[7]
	200	1800	24.4	1380	24.8	[19]
	67	1839	25	1380	33	[7]
	91	1877	20	1380	33	[7]
	200	2000	40.1	1380	20.2	[19]
	75	2059	20	1380	33	[7]
	65	2110	25	1380	33	[7]
	58	2111	23	1380	33	[7]
		2230	21.71	1383	24.71	[38]
	200	2300	22.8	1380	39.2	[19]
	59	2520	25	1380	33	[7]
	69	2523	30	1380	33	[7]
	75	2628	26	1380	33	[7]
	50	2630	30	1380	33	[7]
	200	2700	24.4	1380	39.2	[19]
	59	2722	27	1380	33	[7]
	95	2772	24	1380	33	[7]
	56	2885	27	1380	33	[7]
	48	2958	30	1380	33	[7]
	55	2986	30	1380	33	[7]
	200	3200	32.9	1380	24.8	[19]
	45	3578	33	1380	33	[7]
	50	3682	36	1380	33	[7]
	51	3734	33	1380	33	[7]

	3880	17.57	1383	23.74	[38]
39	3894	35	1380	33	[7]
48	3913	38	1380	33	[7]
39	3937	35	1380	33	[7]
28.36	4011	16.87	1380	18.65	[39]
12	4100	49.9	1380		[31]
39	4390	38	1380	33	[7]
200	4900	40.1	1380	24.8	[19]
200	4900	32.9	1380	39.2	[19]
50	4972	40	1380	33	[7]
40	5093	40	1380	33	[7]
39	5112	40	1380	33	[7]
30	5119	50	1380	33	[7]
32	5356	44	1380	33	[7]
11	5700	64.4	1380		[31]
	6700	32.68	1379	18.83	[38]
5.1	7100	42.1	1930	21	[32]
200	7400	40.1	1380	39.2	[19]
19.49	7412	24.54	1380	18.65	[39]
30	8596	60	1380	33	[7]
10.5	9800	49.8	1380		[31]
	9990	24.68	1379	14.36	[38]
	10,480	60.35	1381	23.66	[38]
8.9	12,500	77.5	1930	21	[32]
	14,530	38.47	1379	14.36	[38]
12.97	16,750	36.88	1380	18.65	[39]
10.5	17,400	72.8	1380		[31]
7.41	18982.46	59.71	1194.2	10	[40]
14	19,700	35.9	1380		[31]
11.3	22,600	113.2	1930	21	[32]
18	22,699	110	1380	33	[7]
11	36,400	57.27	1380	14.2	[41]
11	37,400	56.75	1380	13.91	[41]
11	44,400	56.73	1380	12.72	[41]
11	44,900	56.9	1380	12.72	[41]
12.5	51,000	72.9	1380		[31]
13.93	52692.03	58.93	1473.25	6	[40]
15.19	58031.59	53.84	2692	5	[40]
7.52	65691.49	69.39	1387.8	6	[40]
6.42	74869.16	74.15	1483	6	[40]
10.15	11231.53	78.37	1306	15	[40]

Reclaimed	6.84	11549.71	79	878	13	[40]
	5.98	11956.52	79.09	1318	15	[40]
	10.21	13450.54	81.89	1365	15	[40]
	10.05	13996.02	81.07	1158	15	[40]
	5.78	15032.87	82.89	1381	15	[40]
	7.66	6070.5	61.27	1225.4	17	[40]
Polyester I400-40 (Recycled)	40	1100	10	1380	36	[23]
Polyester I400-30 (Recycled)	30	1500	14	1380	36	[23]
Polyester I600-30 (Recycled)	33	2400	20	1380	36	[42]
Hollow Polyester	6.44	15113.35	72.02	1440.4	12	[40]
30% Hollow PET 45% PET 25% Bi-component PET	27.48	4108	16.93	1142	15.94	[4]
	23.87	5337	19.49	1142	15.94	[4]
	24.09	5757	21.07	1142	15.94	[4]
	20.69	7029	22.48	1142	15.94	[4]
	20.76	7319	24.45	1142	15.94	[4]
	20.32	7498	23.54	1142	15.94	[4]
	19	7530	26.71	1142	15.94	[4]
	18.43	9829	27.54	1142	15.94	[4]
	16.85	10,181	27.61	1142	15.94	[4]
	13.31	12,868	34.95	1142	15.94	[4]
	15.46	13,397	30.94	1142	15.94	[4]
	14.27	14,989	35.56	1142	15.94	[4]
	14.15	15,414	35.87	1142	15.94	[4]
	11.14	19,733	45.56	1142	15.94	[4]
	10.43	20,474	44.6	1142	15.94	[4]
Polypropylene	12.45	30,000	110.04	910	63.4	[17]
Polylactic Acid (PLA)	12.22	23,400	92.47	1240	61.8	[17]
Rock wool		3380	36.5	1380	15	[6]
		3560	36.5	1380	15	[6]
		3860	40.1	1380	15	[6]
		5600	69	1380	18	[6]
		6890	68	1380	17	[6]
		8690	73	1380	17	[6]

	35	10,100	29.7	1380	10	[29]
	30	13,500	32.1	1380	10	[29]
	43	15,100	38.4	1380	10	[29]
	35	15,600	40.2	1380	10	[29]
	27	21,600	42.8	1380	10	[29]
	28	25,100	46.2	1380	10	[29]
	21	46,000	78.4	1380	10	[29]
	25	63,400	88.4	1380	10	[29]
	24	69,400	97	1380	10	[29]
	20	77,290	110	1380	10	[29]
Sheep's Wool	25	720	10	1310	28	[10,43]
	100	720	9	1310	22	[10,43]
	75	1369	18	1310	35	[10,43]
	75	1469	18	1310	28	[10,43]
	100	1550	15	1310	28	[10,43]
	75	2338	18	1310	22	[10,43]
	25	3300	38	1310	35	[10,43]
	100	4000	22	1310	22	[10,43]
	25	8000	47	1310	28	[10,43]
	100	8200	47	1310	28	[10,43]
	25	16,000	98	1310	35	[10,43]
	100	16,700	99	1310	35	[10,43]
	25	20,000	75	1310	28	[10,43]
(Bonded batt)	22	800	10	1310	25	[10,43]
(Bonded batt)	35	800	10	1310	25	[10,43]
(Bonded batt)	45	800	10	1310	25	[10,43]
(Bonded batt)	75	1200	12	1310	22	[10,43]
(Needle punched batt)	40	1950	40	1310		[22]
	40	2100	40	1310		[22]
	60	2250	40	1310		[22]
	23	8000	47	1310	28	[10,43]
Yucca fibre	30	17,730	200	1312	130.8	[44]
	15	21,533	200	1312	130.8	[44]

Table 4
General Fibre Properties.

Fibre Type	Fibre diameter(μm)	Density(kg/m^3)	References
Acrylic (>85% acrylonitrile)	11 – 24	1110	[18]
Bagasse	20	550 – 1250	[45,34]
Bamboo	90 – 425	575	[45,34]
Carbon	5 – 7	1550 – 1780	[46,47]
Coir (Natural)	100 – 460	537 – 1460	[48,25,22,45,47]
Coir (Industrial Prepared)	252	821	[22]
Date Palm	420	930	[28]
E-Glass	17	2550	[47]
Flax	3 – 600	1120 – 1500	[49,50,46,45,47]
Glass	9 – 10.9	2070 – 2500	[14,46,1,32,29,33]
Hemp Batts	93.9	–	[50,51]
Hemp	5 – 500	1500	[14,45,47]
Jute Carded	62.1	1040	[50,51,46]
Jute raw fibre	25 – 200	1040 – 1500	[49,50,51,46,34,47]
Kapok	15 – 23	370	[35]
Kenaf	12.81 – 110	1400	[22,45,52]
Kevlar	12	1440	[47,20]
Nylon	52 – 64	1100 – 1380	[18]
Oil Palm EFB	150 – 500	700 – 1550	[47]
PP	19 – 50	886 – 926	[14,18]
PLA (18% Hollow)	42	1300	[14]
Pineapple Leaf	20 – 80	–	[47]
Polyester	15 – 75	1142 – 1930	[1,32,19,7,31,4,18]
Polyimide	50	1410	[1,53]
Polypropylene	63.4	910	[17]
Polylactic Acid (PLA)	61.8	1240	[17]
Quill (Pulverized)	10 – 40	–	[45]
Raw cotton	8 – 38	1500 – 1600	[50,34,18,45,47]
Ramie	24 – 37	1090–1550	[49,50,46,34,45]
Rice Paddy	8 – 20	–	[45]
Rock Wool	1 – 10	1380	[16,29,42]
Sheep Wool	14 – 63	1310	[50,51,10,22,43,18,45]
Sisal	50 – 213	700 – 1500	[49,50,51,34,47]
Wood	5 – 38	–	[45]
Wool batts	63	–	[50,51]
Yucca	130.8	1312	[44]

since these results are contrary to the prevailing trend demonstrated by the majority of experimental results presented in the literature.

Table 4, offers a comprehensive list of fibre diameter ranges and fibre densities. This data is essential for the accurate prediction of the airflow resistivity of a poroelastic fibrous material. Although this data is essential for accurately predicting the airflow resistivity, it is unfortunately aften not supplied.

Table 3, Table 4 are intended to provide a designer with a starting place when doing prototyping. These tables give a good indication of the performance of different fibre types and also illustrates the effect fibre diameter and bulk density have on airflow resistivity, which is fundamental to the materials ability to absorb sound.

2.3. Development of an airflow resistivity model

Due to the lack of universal accuracy, with regards to different fibrous materials, as depicted in Table 2, the authors attempted to develop a model that could be used to predict the airflow resistivity of any fibre type. Table 2, demonstrates that the currently available models are only effective on a limited range of fibres. In most cases, the presented models can only accurately predict the sound absorption coefficient of one fibre type. There are however a few acceptations to this, such as the Ballagh model, that can predict the airflow resistivity of several fibre types with relatively good accuracy. Never the less, there is space for improvement. The improvement can come through using the available data of many different fibre types to develop an airflow resistivity model. This is possible since the effect of fibre cross-sectional shape does not influence the material's resistance to flow when the aspect ratio of the cross-section is less than 3:1 [54]. This is the case for fibrous sound-absorbing materials since continues fibres are used in the manufacturing of sound-absorbing materials [20].

The data used to develop the model in this paper was obtained from Table 3. A subset consisting of 167 samples of data from Table 3 was extracted based on strict criteria. The data had to be original, hence predicted values were not used. Also, the data had to follow existing knowledge with regards to performance (e.g. increase in bulk density causes an increase in airflow resistivity). Once the subset of data had been extracted the data points were plotted. Thereafter, outliers in the data were identified and removed from the data set. Once the data set had been cleaned up MATLAB was used to fit a least-square regression power function to the data, as seen in Fig. 1. The curve had an R^2 (coefficient of determination) value of 0.9654, which means that 96.54% of the total data variance is explained by the best-fit regression model. Also, the power function coefficients had a confidence bound of 95%.

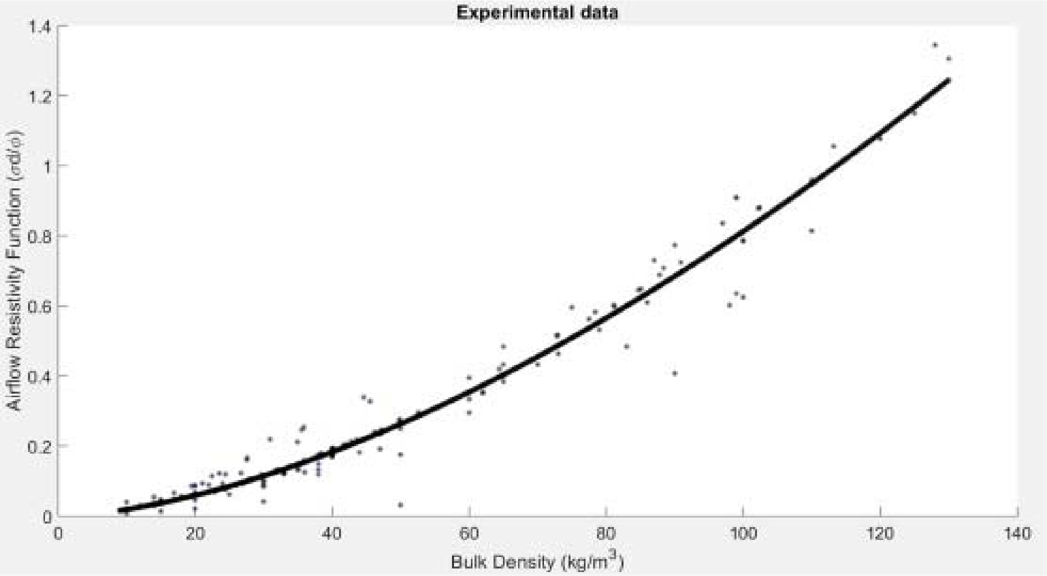

Fig. 1. Power function fit to experimental data.

The predictive model that was derived from Fig. 1 is depicted below in Eq. (2):

$$\sigma = \frac{455.7\phi}{d}\rho_B^{1.626} \tag{2}$$

where δ is the airflow resistivity, is ϕ the porosity of the absorber, d is the fibre diameter and p_B is the bulk density of the absorber. The units of the fibre diameter are *µm*, and the units of the bulk density are kg / m^3, this will give the airflow resistivity the unit $Pa.s/m^2$.

2.4. Benchmarking the development model

After the model had been developed it was necessary to benchmark the model using an independent data set in order to determine the model's accuracy. The data set used to test the developed model was a subset consisting of 24 samples of data derived from Table 2. This subset of data was randomly chosen and consisted of polyester, glass, cotton, coir and date palm fibres.

The airflow resistivity models used to benchmark the model developed in this study were selected based on their prediction accuracy. Therefore, the model developed in this paper was benchmarked against the four best performing models, as evaluated in Table 2. The prediction accuracy was determined using three criteria, firstly, the lowest average percentage error predicted value, secondly, the lowest minimum percentage error predicted value and thirdly, the maximum percentage error predicted value, for all samples tested.

From Table 5, it is evident that the airflow resistivity model developed outperforms the best current available models with regards to all three criteria. Furthermore, the models in Table 5 were evaluated against all the original data, 194 samples, in Table 3. It was found that the developed model predicted the airflow resistivity with an average percentage error of 3.23% lower than the lowest prediction produced by the currently available modes.

Table 5
Accuracy of Airflow Resistivity Models (Subset of data).

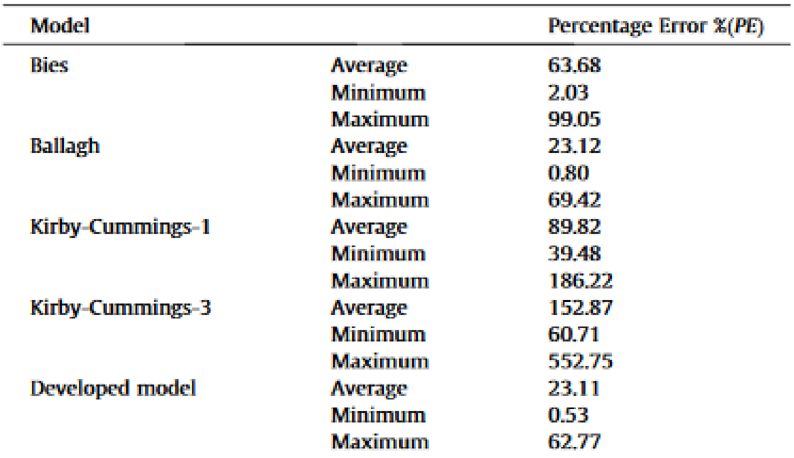

Model		Percentage Error %(*PE*)
Bies	Average	63.68
	Minimum	2.03
	Maximum	99.05
Ballagh	Average	23.12
	Minimum	0.80
	Maximum	69.42
Kirby-Cummings-1	Average	89.82
	Minimum	39.48
	Maximum	186.22
Kirby-Cummings-3	Average	152.87
	Minimum	60.71
	Maximum	552.75
Developed model	Average	23.11
	Minimum	0.53
	Maximum	62.77

After a careful analysis of the predicted results produced by the model developed in this work, it was found that there is no correlation between percentage error and material properties such as bulk density and fibre diameter. This was established by grouping, into two separate groups, all the materials that produced the lowest percentage error and the highest percentage error. It was found that the range of bulk density and fibre diameter that produced the lowest percentage error coincided with the range that produced the highest percentage error.

2.5. The prediction of the sound absorption coefficient

The need for the airflow resistivity of a poroelastic material stems from the desire to understand the effect these materials have on the noise level. As an example, the poroelastic materials (headliner, carpet etc.) implemented in the cabin of a vehicle have a direct effect on the sound pressure level (SPL's) within the vehicle cabin (more information on this subject can be found in [2]). These materials have the ability to reduce the SPL's within the vehicle cabin. The amount by which the material can reduce the SPL's is dependent on the materials sound absorption coefficient, hence, is an important material property to have during the early design stage as discussed in section 2 of this paper. The sound absorption coefficient can be predicted by making use of the airflow resistivity of the material. The equation to determine the sound absorption coefficient is given by the following:

$$\alpha = 1 - \left| \frac{Z_s - \rho_0 c_0}{Z_s + \rho_0 c_0} \right|^2 \tag{3}$$

$$Z_s = -iZ_c \coth(k_c d) \tag{4}$$

where α is the sound absorption coefficient, Z_8 is the surface impedance, and Z_c is the characteristic impedance, k_c is the characteristic wavenumber, c_0 is the speed of sound through air, p_0 is the density of air and d is the thickness of the composite [22]. The characteristic impedance and the characteristic wavenumber can be determined through the following equations:

$$Z_c = \rho_0 c_0 \left[1 + c_1 \left(\frac{\rho_0 f}{\sigma} \right)^{-c_2} - i c_3 \left(\frac{\rho_0 f}{\sigma} \right)^{-c_4} \right] \tag{4}$$

$$k_c = \frac{\omega}{c_0} \left[c_5 \left(\frac{\rho_0 f}{\sigma} \right)^{-c_6} - i c_7 \left(\frac{\rho_0 f}{\sigma} \right)^{-c_8} \right] \tag{5}$$

where w is the angular frequency, f is the frequency, δ is the airflow resistivity of the material, and c_i (with $i = 1 \cdots 8$) are numerical coefficients as described in [55]. A detailed review with regards to the available sound absorption models can be found in [56].

It should be noted that there is still much work that needs to be done on widening the scope and improving the accuracy of the current empirical sound absorption coefficient models, therefore, caution should be used when implementing such models into FEA software.

3. Conclusion

This research was aimed at providing designers with a reliable source of information, with regards to acoustic materials, that can be used for preliminary design purposes. In so doing, the accuracy of many available airflow resistivity models were tested and a database, of acoustic material properties, was subsequently established. Also, a new airflow resistivity model was developed and benchmarked against the current best models available. Based on this new model, it was found that the percentage error and material properties have no visible correlation, to the author's surprise. This may be attributed to the reason that the predictive model's major errors can only come from two main sources 1) the fibre diameter and materials bulk density ranges (meaning that the model is only accurate within a specific range) and 2) inaccuracies in measured data. It was shown that the range did not influence the percentage error, hence, the majority of high percentage errors must come from inaccuracies in the data presented in the available literature. However, a point of error could be that a considerable portion of journal papers cited in this work reported mean fibre diameters. This could be a source of error since the predictive models are very sensitive to fibre diameter. Therefore, it is advised that when attempting to use these predictive models the mean fibre diameter is not used. Since for accurate results, it is imperative to use the actual mean fibre diameter of the specific sample of sound-absorbing material being developed.

In conclusion, it should be noted that the majority of the available literature, with regards to the sound absorption properties of fibrous materials, omit the fibre diameter, bulk density and/or the airflow resistivity, when reporting on the acoustic performance such as the sound absorption coefficient. The reason for this may be due to a lack of available test equipment. This makes it particularly difficult to test and use the developed airflow resistivity models. Also, although there has been much development in natural fibre environmentally friendly materials in recent years, surprisingly; the research shows inadequate availability of data with regards to the airflow resistivity of these materials, as is evident in Table 3. Therefore, the following points are proposed for future work that can be undertaken to improve this body of knowledge.

- Comprehensive testing of acoustic materials (natural and synthetic) needs to be performed and reported on.

- The presented data should include, sound absorption coefficients, airflow resistivity values, material bulk densities, mean fibre diameters of each sample and porosity values.
- The testing should be done in a systematic way to capture the affects bulk density, fibre diameter, material thickness and porosity have on the airflow resistivity and sound absorption coefficient. This can be achieved by varying each parameter a sufficient number of times.
- Thereafter, a comprehensive database of acoustic material properties can be compiled. This will be of great benefit to designers.
- Once a comprehensive error-free database is available accurate predictive models can be developed and be used by designers with confidence.

Funding

This research did not receive any specific grant from funding agencies in the public, commercial, or not-for-profit sectors.

CRediT authorship contribution statement

R.K. Dunne: Conceptualization, Methodology, Investigation, Writing - original draft. **D.A. Desai:** Supervision, Writing - review & editing. **P.S. Heyns:** Supervision, Writing - review & editing.

Declaration of Competing Interest

The authors declare that they have no known competing financial interests or personal relationships that could have appeared to influence the work reported in this paper.

References

[1] Wu, R. and D. Herrin, Utilization of Empirical Models to Determine the Sound Absorption and Bulk Properties of Compressed Materials. 2017.
[2] Dunne RK, Desai DA, Sadiku R. Investigation and development of a numerical tool for the prediction and influence of natural fibre poroelastic trim behaviour on automotive cabin noise. Cogent Eng 2018;5(1):1548992.
[3] Jackson GW, James DF. The permeability of fibrous porous media. Can J Chem Eng 1986;64:364–74.
[4] Yang T et al. Study on the sound absorption behavior of multi-component polyester nonwovens: experimental and numerical methods. Text Res J 2019;89(16):3342–61.
[5] Carman P. Flow of gases through porous media. NY: Academic Press Incorporated; 1956.
[6] Bies DA, Hansen C. Flow resistance information for acoustical design. Applied Acoustics - APPL ACOUST 1980;13:357–91.
[7] Garai M, Pompoli F. A simple empirical model of polyester fibre materials for acoustical applications. Appl Acoust 2005;66:1383–98.
[8] X. Tang X. Yan Airflow resistance of acoustical fibrous materials: Measurements, calculations and applications Journal of Industrial Textiles 2018 152808371880571
[9] Bies, DA. and Hansen, CH., Engineering Noise Control Theory and Practice. 3rd ed. 2003: Spon Press. 733.
[10] Ballagh KO. Acoustical Properties of Wool. Appl Acoust 1996;48(2):101–20.
[11] Tarnow V. Airflow resistivity of models of fibrous acoustic materials. Acoust Soc Am

1996;100(6):3706–13.
[12] Kirby R, Cummings A. Prediction of the bulk acoustic properties of fibrous materials at low frequencies1A shorter version of this paper was presented at the EuroNoise Conference, Lyon, France, 21–23 March 19951. Appl Acoust 1999;56(2):101–25.
[13] Mechel, FP., Formulas of Acoustics. 2nd ed. 2002: Springer. 1275.
[14] Yilmaz, ND., Acoustic Properties of Biodegradable Nonwovens, in Textile Technology Management. 2009, North Carolina State University. p. 297.
[15] Kino N, Ueno T. Experimental determination of the micro- and macrostructural parameters influencing the acoustical performance of fibrous media. Appl Acoust 2007;68(11):1439–58.
[16] Soriano J et al. New absorbent material acoustic based on kenaf's fibre. Materiales de Construccion 2010;60.
[17] Yilmaz N et al. Effects of porosity, fiber size, and layering sequence on sound absorption performance of needle-punched nonwovens. J Appl Polym Sci 2011;121:3056–69.
[18] Manning J, Panneton R. Acoustical model for Shoddy-based fiber sound absorbers. Text Res J 2013;83(13):1356–70.
[19] Pelegrinis MT, Horoshenkov KV, Burnett A. An application of Kozeny-Carman flow resistivity model to predict the acoustical properties of polyester fibre. Appl Acoust 2016;101:1–4.
[20] Arenas J, Crocker M. Recent trends in porous sound-absorbing materials. Sound Vib 2010;44:12–7.
[21] Alba J et al. An electroacoustic method for measuring airflow resistivity of porous sound-absorbing materials. Appl Acoust 2019;150:132–7.
[22] Berardi U, Iannace G. Predicting the sound absorption of natural materials: Best-fit inverse laws for the acoustic impedance and the propagation constant. Appl Acoust 2017;115:131–8.
[23] del Rey R et al. Evaluation of two alternative procedures for measuring airflow resistance of sound absorbing materials. Archiv Acoust 2013;38(4):547–54.
[24] Taban E et al. Comparison of acoustic absorption characteristics of coir and date palm fibers: experimental and analytical study of green composites. Int J Environ Sci Technol 2020;17(1):39–48.
[25] Fouladi M, Ayub M, Mohd Nor J. Analysis of coir fiber acoustical characteristics. Appl Acoust 2011;72:35–42.
[26] Taban E et al. Acoustic absorption characterization and prediction of natural coir fibers. Acoustics Australia 2019.
[27] Gómez Méndez, T., NATURAL FIBERS-BASED NONWOVENS OBTAINED BY CHEMICAL BONDING FOR POTENTIAL SOUND ABSORPTION APPLICATIONS. 2020.
[28] Taban E et al. Experimental and mathematical survey of sound absorption performance of date palm fibers. Heliyon 2019;5:e01977.
[29] Komatsu T. Improvement of the Delany-Bazley and Miki models for fibrous sound-absorbing materials. Acoust Sci Technol 2008;29.
[30] Oliva D, Hongisto V. Sound absorption of porous materials – accuracy of prediction methods. Appl Acoust 2013;74(12):1473–9.
[31] Kino N, Ueno T. Improvements to the Johnson-Allard model for rigid-framed fibrous materials. Appl Acoust 2007;68:1468–84.
[32] Schiavi, A., P. Miglietta, and C. Guglielmone, Considerations on the airflow resistivity measurement of porous and fibrous materials as function of temperature. Vol. 31. 2009.
[33] Panneton R, Atalla N. An efficient finite element scheme for solving the three-dimensional poroelasticity problem in acoustics. J Acoust Soc Am 1997;101 (6):3287–98.

[34] Dunne R et al. A review of natural fibres, their sustainability and automotive applications. J Reinf Plast Compos 2016;35(13):1041–50.
[35] Xiang H-F et al. Investigation on sound absorption properties of kapok fibers. Chin J Polymer Sci (English Edition) 2012;31:521–9.
[36] Sambu M et al. Investigation on acoustical and physical characteristics of Kenaf Intermix with Natural Rubber. Int Rev Mech Eng (IREME) 2016;10:284.
[37] Saba N, Jawaid M, Tahir PM. Mechanical properties of kenaf fibre reinforced polymer composite: a review. Constr Build Mater 2014;76:87–96.
[38] Hurrell A, Horoshenkov K, Pelegrinis MT. The accuracy of some models for the airflow resistivity of nonwoven materials. Appl Acoust 2018;130:230–7.
[39] Yang T et al. A study of some airflow resistivity models for multi-component polyester fiber assembly. Appl Acoust 2018;139:75–81.
[40] Kannan, A.J., P. Banks-Lee, and M. Jones, Acoustical absorptive properties of nonwovens. 2005: p. 9-17.
[41] Kino N, Ueno T. Evaluation of acoustical and non-acoustical properties of sound absorbing materials made of polyester fibres of various cross-sectional shapes. Appl Acoust 2008;69:575–82.
[42] Bonfiglio P, Pompoli F, Shravage P. Quasistatic evaluation of mechanical properties of poroelastic materials: static and dynamic strain dependence and in vacuum tests. J Acoust Soc Am 2008;123:3037.
[43] Hillbrick, L., Fibre properties affecting the softness of wool and other keratins. 2013.
[44] Soltani P et al. Experimental and computational investigation of sound absorption performance of sustainable porous material: Yucca Gloriosa fiber. Appl Acoust 2019;157.
[45] Arenas J. and F. Eco-Materials with Noise Reduction Properties: Asdrubali; 2017.
[46] Yang W, Li Y. Sound absorption performance of natural fibers and their composites. Sci China Technol Sci 2012;55.
[47] Md Akil H et al. Kenaf fiber reinforced composites: a review. Mater Des 2011;32:4107–21.
[48] Rey R et al. Technical notes: evaluation of two alternative procedures for measuring airflow resistance of sound absorbing materials. Archiv Acoust 2013;38:547–54.
[49] Mamtaz H et al. Acoustic absorption of natural fiber composites. J Eng 2016;2016:1–11.
[50] Oldham D, Egan C, Cookson R. Sustainable acoustic absorbers from the biomass. Applied Acoustics - APPL ACOUST 2011;72:350–63.
[51] Borlea, et al. Innovative use of sheep wool for obtaining materials with improved sound-absorbing properties. Materials 2020;13:694.
[52] Nirmal U, Lau S, Hashim J. Interfacial adhesion characteristics of kenaf fibres subjected to different polymer matrices and fibre treatments. J Compos 2014;2014.
[53] Yan, Y., Developments in fibers for technical nonwovens. 2016. p. 19-96.
[54] Labrecque, RP., An Investigation of the Effects of Fibre Cross Sectional Shape on the Resistance to Flow of Fluids Through Fiber Mats. 1967, The Institute of Paper Chemistry: Wisconsin. p. 94.
[55] Berardi, U., Determination through an inverse method of the acoustic impedance and the propagation constant for some natural fibers, in inter. noise 2015. 2015: San Francisco, California, USA.
[56] Dunne R, Desai D, Sadiku R. A review of the factors that influence sound absorption and the available empirical models for fibrous materials. Acoust Australia 2017;45.